Physics Letters B 750 (2015) 384–389

Contents lists available at ScienceDirect

Physics Letters B

www.elsevier.com/locate/physletb

Family gauge boson production at the LHC

Yoshio Koide [a], Masato Yamanaka [b,*], Hiroshi Yokoya [c,d]

[a] Department of Physics, Osaka University, Toyonaka, Osaka 560-0043, Japan
[b] Kobayashi–Maskawa Institute for the Origin of Particles and the Universe (KMI), Nagoya University, Nagoya 464-8602, Japan
[c] Quantum Universe Center, KIAS, Seoul 130-722, Republic of Korea
[d] Theory Center, KEK, Tsukuba 305-0801, Japan

ARTICLE INFO

Article history:
Received 23 July 2015
Received in revised form 10 September 2015
Accepted 10 September 2015
Available online 25 September 2015
Editor: J. Hisano

ABSTRACT

Family gauge boson production at the LHC is investigated according to a $U(3)$ family gauge model with twisted family number assignment. In the model we study, a family gauge boson with the lowest mass, $A_1{}^1$, interacts only with the first generation leptons and the third generation quarks. (The family numbers are assigned, for example, as $(e_1, e_2, e_3) = (e^-, \mu^-, \tau^-)$ and $(d_1, d_2, d_3) = (b, d, s)$ [or $(d_1, d_2, d_3) = (b, s, d)$].) In the model, the family gauge coupling constant is fixed by relating to the electroweak gauge coupling constant. Thus measurements of production cross sections and branching ratios of $A_1{}^1$ clearly confirm or rule out the model. We calculate the cross sections of inclusive $A_1{}^1$ production and $b\bar{b}\,(t\bar{t})$ associated $A_1{}^1$ production at $\sqrt{s} = 14$ TeV and 100 TeV. With the dielectron production cross section, we discuss the determination of diagonalizing matrix of quark mass matrix, U_u and U_d, respectively.

1. Introduction

One of the most challenging subjects in particle physics is to understand the origin of "flavor". It seems to be very attractive to understand "families" ("generations") in quarks and leptons from concept of a symmetry [1]. Besides, in the standard model (SM) of quarks and leptons, a degree of the freedom which is not yet accepted as a gauge symmetry is only that of the families. Usually, since it is considered that an energy scale of the family symmetry breaking is extremely high (e.g. a GUT scale), such family gauge models cannot be tested by terrestrial experiments. In addition, due to large degrees of freedoms in the models, both an identification of each model and shedding light on model structures are quite difficult. However, if a family gauge model is realized at the TeV scale and possesses a certain degree of freedom for a clear purpose, it is worth investigating experimental verifications of such family gauge model seriously.

Against such conventional family gauge boson (FGB) models, recently, a model (Model A) with a considerably small FGB mass scale has been proposed by Sumino [2]. Sumino has noticed a problem in a charged lepton mass relation [3],

$$K \equiv \frac{m_e + m_\mu + m_\tau}{\left(\sqrt{m_e} + \sqrt{m_\mu} + \sqrt{m_\tau}\right)^2} = \frac{2}{3}. \tag{1.1}$$

The relation is satisfied by the pole masses [i.e. $K^{pole} = (2/3) \times (0.999989 \pm 0.000014)$], but not so well satisfied by the running masses [i.e. $K(\mu) = (2/3) \times (1.00189 \pm 0.00002)$ at $\mu = m_Z$]. The running masses $m_{e_i}(\mu)$ are given by [4]

$$m_{e_i}(\mu) = m_{e_i}\left[1 - \frac{\alpha_{em}(\mu)}{\pi}\left(1 + \frac{3}{4}\log\frac{\mu^2}{m_{e_i}^2(\mu)}\right)\right]. \tag{1.2}$$

If the family-number dependent factor $\log(m_{e_i}^2/\mu^2)$ in Eq. (1.2) is absent, then the running masses $m_{e_i}(\mu)$ also satisfy the formula (1.1). In order to understand this situation, Sumino has proposed a U(3) family gauge model [2] so that a factor $\log(m_{e_i}^2/\mu^2)$ in the QED correction for the charged lepton mass m_{e_i} $(i = 1, 2, 3)$ is canceled by a factor $\log(M_{ii}^2/\mu^2)$ in a corresponding diagram due to the FGBs. Here, the masses of FGBs $A_i{}^j$, M_{ij}, are given by

$$M_{ij}^2 = k(m_{e_i}^n + m_{e_j}^n), \tag{1.3}$$

* Corresponding author.
E-mail addresses: koide@kuno-g.phys.sci.osaka-u.ac.jp (Y. Koide), yamanaka@eken.phys.nagoya-u.ac.jp (M. Yamanaka), hyokoya@kias.re.kr (H. Yokoya).

http://dx.doi.org/10.1016/j.physletb.2015.09.024

where k is a constant with dimension of (mass)$^{2-n}$. The cancellation mechanism holds in any cases of n in Eq. (1.3), because $\log M_{ii}^n = n \log M_{ii}$, although, in Model A, a case $n = 1$ has been taken. The cancellation condition requires the following relation between the family gauge coupling constant g_F and QED coupling constant e,

$$\left(\frac{g_F}{\sqrt{2}}\right)^2 = \frac{2}{n}e^2 = \frac{4}{n}\left(\frac{g_w}{\sqrt{2}}\right)^2 \sin^2\theta_w. \tag{1.4}$$

Here θ_w is the Weinberg angle. Hence, in the FGB model we consider, the family gauge coupling constant g_F is fixed by Eq. (1.4).

Next we see the reason why FGBs are not so heavy. Since we consider $M_{ii}^2 \propto m_{e_i}^n$, the magnitude of M_{ii} itself is not important for the cancellation mechanism, and only the linear form of $\log(M_{ii}/\mu)$ is essential, because $\log M_{ii}^2 = n \log m_{e_i} + const.$ However, the cancellation mechanism holds only in the one-loop diagram with FGBs. Contributions from two loop diagrams include other forms (e.g., $\log^2 M_{ii}$ and so on) in addition to the form $\log M_{ii} + const.$ Therefore, if FGBs are too heavy, the two-loop diagrams cannot be negligible, so that the cancellation mechanism is violated sizably. In other words, we cannot take the symmetry braking scale Λ too large. A speculation in Refs. [2,5] also supports that the breaking scale should be intermediate scale between the electroweak and GUT scale. The author claims that the family gauge symmetry is an effective theory and must be embedded into a more fundamental symmetry at some scale. The scale is derived to be 10^2–10^3 TeV from the realization of the cancellation relation (1.4) without fine tuning (details are given in Refs. [2,5]). In this work, based on these reasons, we suppose the breaking scale to be 10^3–10^4 TeV. Let us take $n = 2$ in Eq. (1.3). (The case with $n = 2$ has been discussed in the Ref. [6].) Then, we obtain $M_{11}/M_{33} \sim m_e/m_\tau$. Since $m_\tau/m_e \simeq 3.5 \times 10^3$, we find $M_{11} \sim$ a few TeV with the assumption of $M_{33} \sim \Lambda \sim 10^4$ TeV. As we show in this study, a search for a FGB with the mass $M_{11} \sim$ a few TeV is within our reach at the LHC.

An evidence of FGB can be indirectly observed from a deviation from the e–μ–τ universality. However, such an observation has large systematic error at present, and, for the time being, the improvement is not so easy. Besides, even if the deviations are found, there exists various interpretations. On the other hand, an observation of new vector bosons which interact with specific family fermions can be a direct evidence at collider experiments. Here we note that, in general, family numbers in the lepton and quark sectors can be assigned individually. As we describe in the next section, in the family gauge model we consider, the lightest FGB couples with only first generation leptons and third generation quarks. Therefore, the FGB has distinguished collider signatures, such as the characteristic production processes and their cross sections, as well as the branching ratios. The complementary check by the measurements of dielectron production cross section and $b\bar{b}\,(t\bar{t})$ associated ${A_1}^1$ production cross sections clearly confirms or rules out the family gauge model. Besides, by measuring the branching ratios of the FGB, we can distinguish whether the signal is from the FGB or not.

This work is organized as follows. First we briefly review our model (Model B) which is an extended version of Model A, in particular, the interactions relevant for the collider phenomenology. Then we comment on the assignment of family number in quark sector with taking into account the observational results of pseudo scalar oscillations. Next, in Section 3, we check current direct bound on ${A_1}^1$ from the data of LHC 8 TeV run. Then, we evaluate the production cross section of ${A_1}^1$ at $\sqrt{s} = 14$ TeV and 100 TeV, and discuss the feasibility of the discovery in future experiments. Finally, Section 4 is devoted to summary and discussion.

2. Family gauge boson model

We describe the interactions and flavor structures in the family gauge model proposed in Ref. [6], which we call Model B, to discuss the collider signatures of the FGBs in the model. Model B is an extended model of the family gauge model proposed in Ref. [2], which we call Model A. Model B improves the shortcomings of Model A, and as a result, characteristic interactions for the FGBs are introduced. We give a brief review on Model B in this section.

In Model A [2], Sumino has assigned the fermions (quarks and leptons) (f_L, f_R) to $(\mathbf{3}, \mathbf{3}^*)$ of U(3), the gauge group of the family gauge symmetry, in order to obtain the minus sign for the cancellation in lepton running masses, i.e., the cancellation between a factor $\log m_{e_i}^2$ and $\log M_{ii}^2$ (see Introduction). Although the assignment successfully brings the cancellation mechanism, it has a shortcoming from the phenomenological point of view: The assignment induces effective quark–quark interactions with $\Delta N_{fam} = 2$ (N_{fam} is family number). It causes a serious conflict with the observed P^0–$\bar{P}^0$ mixings ($P = K, D, B, B_s$). Therefore, in the Model B, only for quark sector, we restore the Sumino's assignment $(q_L, q_R) \sim (\mathbf{3}, \mathbf{3}^*)$ of U(3) to the normal assignment $(q_L, q_R) \sim (\mathbf{3}, \mathbf{3})$, in order to suppress the unwelcome quark–quark interactions with $\Delta N_{fam} = 2$. We note that, in the quark sector, we do not need such cancellation mechanism as in the charged lepton masses. On the other hand, the idea of cancellation mechanism is inherited in the lepton sector from Model A. Thus, we adopt $(\ell_L, \ell_R) \sim (\mathbf{3}, \mathbf{3}^*)$ [2] for the lepton sector, so that the relations (1.3) and (1.4) hold for the cancellation mechanism. As a result, the FGB interactions with quarks and leptons are given as follows:

$$\mathcal{H}_{fam} = \frac{g_F}{\sqrt{2}}\left[\sum_{\ell=\nu,e}\left(\bar{\ell}_L^i \gamma_\mu \ell_{Lj} - \bar{\ell}_{Rj}\gamma_\mu \ell_R^i\right) + \sum_{q=u,d}(U_q^*)_{ik}(U_q)_{jl}(\bar{q}_k \gamma_\mu q_l)\right](A_i^{\ j})^\mu. \tag{2.1}$$

We note that the U(3) assignment for fermions is not anomaly free in both Models A and B. In order to avoid this shortcoming, we tacitly assume an existence of heavy leptons in the lepton sector.

Furthermore, in the present paper, we discuss the case $n = 2$, only the case which can give $M_{11} \sim 1$ TeV [6]. Then, the value of g_F is fixed as follows:

$$\left.\frac{g_F}{\sqrt{2}}\right|_{n=2} = e = 0.30684. \tag{2.2}$$

In Model B as well as in Model A, the FGB mass matrix is diagonal in a flavor basis in which the charged lepton mass matrix M_e is diagonal. There is no family number violation at the tree level in the lepton sector. However, in general, there is a mixing between the family number basis and the mass basis in the quark sector. In Eq. (2.1), U_q is the diagonalizing matrix for the quark mass matrix M_q, and the Cabibbo–Kobayashi–Maskawa (CKM) [7] quark mixing matrix V_{CKM} is given by $V_{CKM} = U_{Lu}^\dagger U_{Ld}$. In this paper, for convenience, we assume the mass matrix is Hermitian, thus $U_{Lq} = U_{Rq} = U_q$. In addition, for numerical estimates, we use an assumption,

$$U_u \simeq \mathbf{1}, \quad U_d \simeq V_{CKM}, \tag{2.3}$$

by considering the observed fact $m_t - m_u \gg m_b - m_d$.

Even if we adopt $(q_L, q_R) \sim (\mathbf{3}, \mathbf{3})$, the observed K^0–$\bar{K}^0$ mixing still puts a severe constraint on the masses M_{ij}. To avoid this constraint, we can take a lower mass only for the FGB which interacts

with the third generation quarks. Hence, a twisted family number assignment,

$$(d_1, d_2, d_3) = (b, d, s) \ \ [\text{or } (d_1, d_2, d_3) = (b, s, d)] \ \text{ vs.}$$
$$(e_1, e_2, e_3) = (e^-, \mu^-, \tau^-) \tag{2.4}$$

has been proposed for the quark sector [6]. In this case, the lightest FGB $A_1{}^1$ interacts with the first generation leptons and the third generation quarks. Thereby, we can safely construct a family gauge model with lower mass scale without conflicting with constraints from the observed P^0–$\bar{P}^0$ mixing [6]. This assignment (2.4) is a key idea to make the FGB model viable at the TeV scale.

3. $A_1{}^1$ production at the LHC

One of the clear observables at collider experiments in the present model is the dielectron resonance via the lightest FGB $A_1{}^1$. The interactions (2.1) indicate that additional important observable is the $A_1{}^1$ production associated with third generation quarks. $A_1{}^1$ mass is obtained by the peak position in the dielectron invariant mass, and $A_1{}^1$ interactions are, in principle, determined by the measurement of the cross sections for these processes. In this section, we evaluate the cross sections at the LHC, and discuss the feasibility of the discovery of $A_1{}^1$ FGB in future collider experiments.

3.1. Branching ratios of the FGB $A_1{}^1$

Prior to calculation of the production rate of $A_1{}^1$ at the LHC, we discuss the decay rates of $A_1{}^1$. Major decay modes of $A_1{}^1$ are $t\bar{t}$, $b\bar{b}$, e^+e^- and $\nu\bar{\nu}$, where $\nu\bar{\nu}$ indicates the sum of the neutrino anti-neutrino pair over the three mass eigenstates. The partial decay width $\Gamma(A_1{}^1 \to f + \bar{f})$ is given by

$$\Gamma(A_1{}^1 \to f + \bar{f}) = \frac{C}{12\pi}\frac{g_F^2}{2} M_{11}\left(1 + \frac{2m_f^2}{M_{11}^2}\right)\sqrt{1 - \frac{4m_f^2}{M_{11}^2}}, \tag{3.1}$$

where C is a factor, $C = 1$ for charged leptons and $C = 3 \times |(U_q)_{1i}|^2$ for the quark pair $\bar{q}_i q_i$. For neutrinos, $C = 1/2$ for Majorana case, while $C = 1$ for Dirac case.

$A_1{}^1$ with its mass lighter than 1 TeV has been already excluded by the direct search at the LHC 8 TeV run (see next subsection). For $M_{11} > 1$ TeV, we can approximate

$$\left(1 + 2m_f^2/M_{11}^2\right)\sqrt{1 - 4m_f^2/M_{11}^2} \simeq 1.$$

With this approximation, the total decay width for $M_{11} > 1$ TeV is given for the case of Majorana neutrinos by

$$\Gamma_{A_{11}} \cong 18.73\,[\text{GeV}]\left(\frac{M_{11}}{1\,\text{TeV}}\right). \tag{3.2}$$

Such a relatively narrow width is one of distinctive features of $A_1{}^1$. The branching ratios are calculated as follows:

$$Br(A_1{}^1 \to t\bar{t}) \simeq Br(A_1{}^1 \to b\bar{b}) \simeq 40\%,$$
$$Br(A_1{}^1 \to e^-e^+) = \frac{2}{15} = 13.3\%,$$
$$Br(A_1{}^1 \to \nu\bar{\nu}) = \frac{1}{15} = 6.7\%, \tag{3.3}$$

while the other decay modes are zero or highly suppressed as long as we employ the naive assumption for the quark mixing matrices in Eq. (2.3).

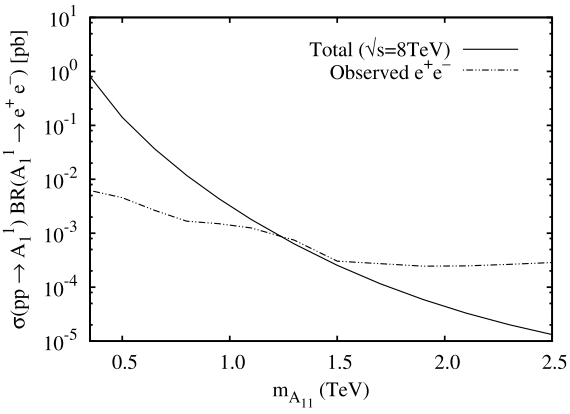

Fig. 1. The cross section of dielectron production via $A_1{}^1$ at $\sqrt{s} = 8$ TeV [solid curve]. Horizontal two-dot chain curve represents the observed 95% C.L. upper limit of the cross section of dielectron resonance [14].

In the case of Dirac neutrinos, the total decay width is given by $\Gamma_{A_{11}} = 19.98\,[\text{GeV}]\,(M_{11}/1\,\text{TeV})$, and the branching ratios are

$$Br(A_1{}^1 \to t\bar{t}) \simeq Br(A_1{}^1 \to b\bar{b}) \simeq 37.5\%,$$
$$Br(A_1{}^1 \to e^-e^+) = Br(A_1{}^1 \to \nu\bar{\nu}) = \frac{1}{8} = 12.5\%, \tag{3.4}$$

with zero or negligibly small ratios for the other modes. The difference between the two cases is due to the number of light neutrinos, since FGBs couple to both the left-handed and right-handed neutrinos. In future, when data of the $A_1{}^1$ production is accumulated, we are able to conclude whether neutrinos are Dirac-type or Majorana-type by measuring the branching ratios of FGBs. Especially, the branching ratio for the invisible decay mode has the largest difference between the two cases.

One of the ingredients to discriminate our scenario and other models is the ratio between branching ratios of e^+e^- and $b\bar{b}$ (or $t\bar{t}$) final states, $\text{Br}(A_1{}^1 \to b\bar{b}(t\bar{t}))/\text{Br}(A_1{}^1 \to e^+e^-) \simeq 3$. This is because that various models possess an extra neutral current, and each model predicts different partial width for each final states e^+e^-, $b\bar{b}$ (or $t\bar{t}$), and so on. We see two examples. One of the natural classes of models that predict an extra neutral current is extra dimension models. An example is the Randall–Sundrum model [8]. The Kaluza–Klein (KK) partner of graviton G_{KK} is a Z' boson like particle, which can produce di-top and di-electron signals. In this model, the ratio is $\text{Br}(G_{\text{KK}} \to t\bar{t})/\text{Br}(G_{\text{KK}} \to e^+e^-) \gtrsim 10^3$ [9]. Another example is the universal extra dimension (UED) model [10]. The second KK partner of $U(1)_Y$ gauge boson $B^{(2)}$ is also a Z' boson like particle, and decays into e^+e^-, $b\bar{b}$ and others. In the UED model, the ratio is $\text{Br}(B^{(2)} \to b\bar{b})/\text{Br}(B^{(2)} \to e^+e^-) \simeq (7\text{–}10)$ [11,12].

3.2. Production rate and discovery significance

Now we evaluate the cross sections of $A_1{}^1$ production, and see the perspective of $A_1{}^1$ direct search at the LHC and future hadron collider experiments. For a reference scenario, first, we take $U_u = \mathbf{1}$ and $U_d = V_{\text{CKM}}$. The quark mixings in the following calculation are $|V_{td}| = 0.00886$, $|V_{ts}| = 0.0405$, and $|V_{tb}| = 0.99914$ [13].

Direct search results for heavy neutral gauge bosons in dilepton final states are reported by the ATLAS and CMS experiments [14,15]. Before we discuss the perspective, we check the current bound on $A_1{}^1$ from the LHC data. Fig. 1 shows the dielectron production cross section via $A_1{}^1$ at $\sqrt{s} = 8$ TeV as a function of the $A_1{}^1$ mass. The cross section is calculated using calcHEP [16]

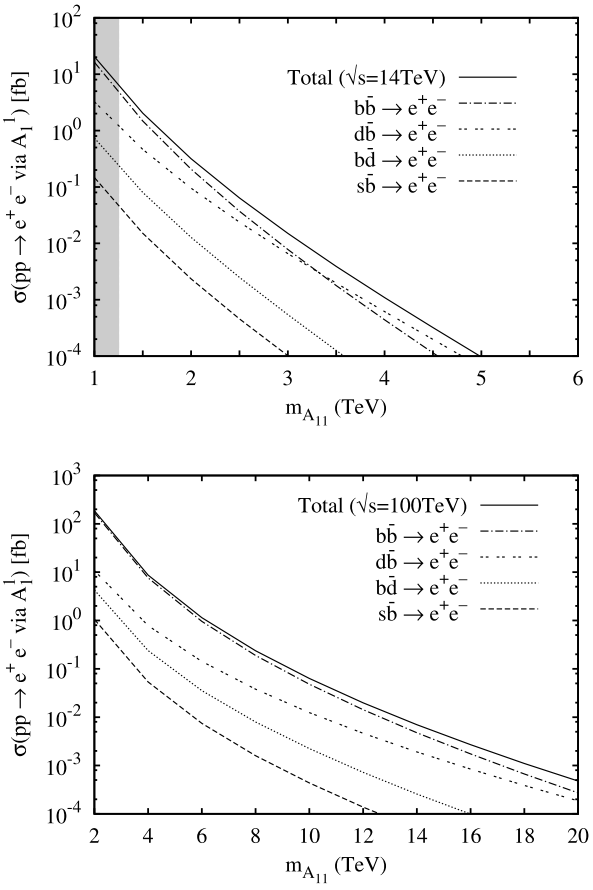

Fig. 2. The cross section of dielectron production via $A_1{}^1$ at $\sqrt{s} = 14$ TeV [top panel] and at $\sqrt{s} = 100$ TeV [bottom panel]. Other curves show partial cross sections for the subprocesses with large contributions. A cut on the invariant mass of the e^+e^- pair is placed as $M_{11} - 1.5\Gamma_{A_{11}} \le m_{ee} \le M_{11} + 1.5\Gamma_{A_{11}}$. Shaded region is ruled out by dilepton search at $\sqrt{s} = 8$ TeV LHC.

with the CTEQ6L parton distribution functions [17]. In the evaluation of $\sigma(pp \to A_1{}^1 \to e^+e^-)$, we apply a cut on the invariant mass of the e^+e^- pair, $M_{11} - 1.5\Gamma_{A_{11}} \le m_{ee} \le M_{11} + 1.5\Gamma_{A_{11}}$. The horizontal curve represents observed 95% C.L. upper limit of the cross section of dielectron resonance with an integrated luminosity 20.3 fb^{-1} [14]. By a comparison of the observed limit and our calculation, the mass limit of $M_{11} \gtrsim 1.25$ TeV is obtained. This is the current lower limit of M_{11} in the scenario with $U_u = \mathbf{1}$ and $U_d = V_{\rm CKM}$.

We are in a position to investigate the feasibility of the $A_1{}^1$ discovery at the future LHC and 100 TeV collider experiments. Fig. 2 shows dielectron production cross section via $A_1{}^1$ at $\sqrt{s} = 14$ TeV [top panel] and at $\sqrt{s} = 100$ TeV [bottom panel]. Solid curve represents the total cross section, and other curves show partial cross sections for the subprocesses with large contributions. Shaded region is excluded by the direct search at the $\sqrt{s} = 8$ TeV run (see Fig. 1).

Here we briefly see each contribution to the dielectron production. The largest contribution almost throughout the mass region we consider comes from $b\bar{b} \to A_1{}^1 \to e^+e^-$, nonetheless b- and $\bar{b}$-quark distributions in a proton are very small. This is because there is no suppression from the off-diagonal elements of the CKM matrix. Similarly the process $d\bar{b} \to A_1{}^1 \to e^+e^-$ also gives large contribution. Compared with the process $b\bar{b} \to A_1{}^1 \to e^+e^-$, the cross section of this process gets suppression by $|(V_{\rm CKM})_{td}|^2$, but enhancement by large distribution of d-quark in a proton. Other processes have small contributions due to both the suppressions from the CKM off-diagonal elements and the low densities of sea quarks in a proton.

Table 1
Significance of the $A_1{}^1$ discovery on 14 TeV LHC run, $S/\sqrt{S+B}$, for integrated luminosity $\mathcal{L} = 300$ fb^{-1} and 3000 fb^{-1}. Here S and B are numbers of signal event and background event, respectively.

M_{11} [TeV]	$\sigma_{\rm BG}$ [pb]	$\frac{S}{\sqrt{S+B}}$ (for 300 fb^{-1})	$\frac{S}{\sqrt{S+B}}$ (for 3000 fb^{-1})
2.0	6.801×10^{-5}	6.859	21.69
2.5	2.084×10^{-5}	2.943	9.306
3.0	7.072×10^{-6}	1.356	4.287
3.5	2.556×10^{-6}	0.653	2.063
4.0	9.580×10^{-7}	0.324	1.025
4.5	3.661×10^{-7}	0.164	0.520
5.0	1.406×10^{-7}	0.084	0.267

Table 2
Significance of the $A_1{}^1$ discovery at 100 TeV collider experiment, $S/\sqrt{S+B}$, for integrated luminosity $\mathcal{L} = 300$ fb^{-1} and 3000 fb^{-1}. Here S and B are numbers of signal event and background event, respectively.

M_{11} [TeV]	$\sigma_{\rm BG}$ [pb]	$\frac{S}{\sqrt{S+B}}$ (for 300 fb^{-1})	$\frac{S}{\sqrt{S+B}}$ (for 3000 fb^{-1})
2.0	2.818×10^{-3}	182.0	575.5
4.0	2.497×10^{-4}	38.97	123.2
6.0	5.428×10^{-5}	14.01	44.32
8.0	1.705×10^{-5}	6.296	19.91
10.0	6.504×10^{-6}	3.211	10.16
12.0	2.811×10^{-6}	1.765	5.580
14.0	1.317×10^{-6}	1.027	3.249
16.0	6.562×10^{-7}	0.625	1.976
18.0	3.370×10^{-7}	0.390	1.233
20.0	1.801×10^{-7}	0.250	0.789

We quantitatively discuss the feasibility of the $A_1{}^1$ discovery. As an indicator of the $A_1{}^1$ discovery reach, we evaluate the significance $S/\sqrt{S+B}$ (Table 1 for the 14 TeV LHC run and Table 2 for 100 TeV collider experiment). Here S and B are the numbers of the dielectron signal and its SM background, respectively. In the evaluation of the significance, we take 300 fb^{-1} and 3000 fb^{-1} as an integrated luminosity. Based on the discussion in Ref. [14], we take the product of the acceptance and efficiency to be 0.6 for each point.

We include only SM Drell–Yan production, $pp \to Z^*/\gamma^* \to e^+e^-$, in the evaluation of the SM background, because this is the dominant contribution in the region of $m_{ee} \gtrsim 2$ TeV (see TABLE V in Ref. [14]). The background cross section is calculated per an energy bin of $3 \times \Gamma_{A_{11}}$ centered at each M_{11}.

Three sigma significance is an important milestone, which implies an "evidence". Table 1 shows that, with the integrated luminosity of 3000 fb^{-1} at $\sqrt{s} = 14$ TeV, the family gauge boson with $M_{11} \lesssim 3.2$ TeV can be identified as an "evidence", and assists the model to be confirmed. Similarly, Table 2 shows that, at $\sqrt{s} = 100$ TeV, the family gauge boson with $M_{11} \lesssim 14$ TeV is within the reach of the "evidence".

One of the key ingredients for the discrimination between our scenario and other scenarios is to check the decay properties of $A_1{}^1$. Since $A_1{}^1$ couples with electron but not with muon and tau lepton, the discovery of dielectron resonance in the absence of dimuon and ditau resonances at the same mass suggests the existence of $A_1{}^1$. Such an unequal rate in the dilepton signal is one of the clear signatures of the model, but not yet a sufficient evidence. We have to check the other specific features of $A_1{}^1$: (i) unequal rates of diquark resonance, i.e., $\mathrm{Br}(A_1{}^1 \to b\bar{b}) \gg \mathrm{Br}(A_1{}^1 \to$ light flavors), e.g., (ii) the ratio between branching ratios of e^+e^- and $b\bar{b}$ final states, $\mathrm{Br}(A_1{}^1 \to b\bar{b})/\mathrm{Br}(A_1{}^1 \to e^+e^-) \simeq 3$. (iii) confirmation of the spin of $A_1{}^1$ by the angular analysis in the dielectron events.

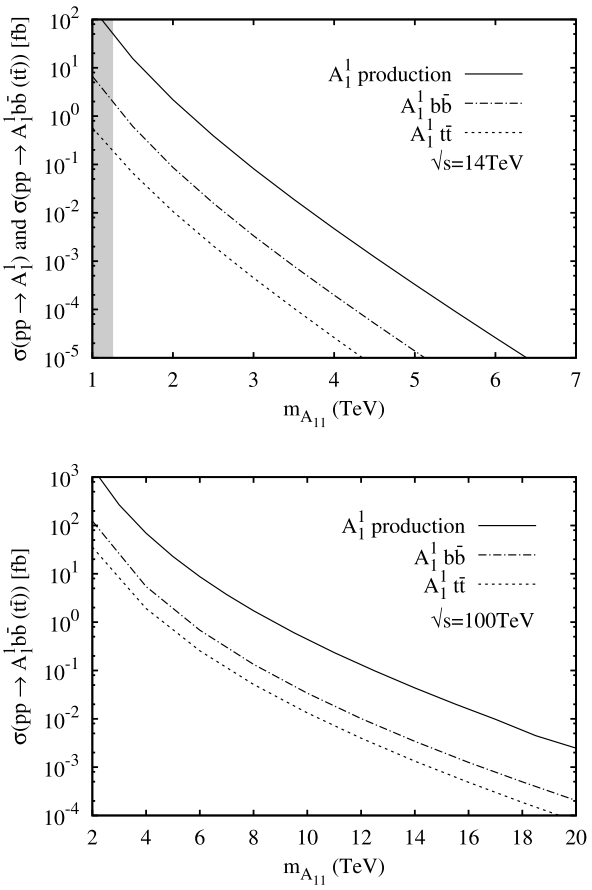

Fig. 3. The cross sections of $A_1{}^1$ direct production and $b\bar{b}$ ($t\bar{t}$) associated productions at $\sqrt{s} = 14$ TeV [top panel] and at $\sqrt{s} = 100$ TeV [bottom panel]. For the $b\bar{b}$ associated production, two cuts are placed: (i) large transverse momentum $p_T^{b(\bar{b})} > 25$ GeV (ii) pseudo-rapidity smaller than $|\eta| < 2.5$. Shaded region is ruled out by the dilepton search at $\sqrt{s} = 8$ TeV LHC.

Another key ingredient for the discrimination and the confirmation of the model is the cross sections of $b\bar{b}$ ($t\bar{t}$) associated $A_1{}^1$ productions. The FGB $A_1{}^1$ interacts with top and bottom quarks, but not with other quarks when we omit the intergenerational mixing. Thus, the cross sections of $A_1{}^1$ production associated with $b\bar{b}$ ($t\bar{t}$) must be larger than that of $A_1{}^1$ production associated with light flavor jets. Thus the measurement of $\sigma(pp \to A_1{}^1 + b\bar{b}\,(t\bar{t}))$ is a nice complementary check of the scenario. Fig. 3 shows the cross sections of the processes $pp \to A_1{}^1$ and $pp \to A_1{}^1 + b\bar{b}\,(t\bar{t})$ at $\sqrt{s} = 14$ TeV [top panel] and at $\sqrt{s} = 100$ TeV [bottom panel], respectively. The events for $b\bar{b}$ associated $A_1{}^1$ production can be safely distinguished from those for the inclusive $A_1{}^1$ production via $b\bar{b}$ annihilation by requiring the b-tagged jets with large transverse momenta. Thus, for the estimation of the cross section, we impose a cut on each b-jet: (i) large transverse momentum $p_T^{b(\bar{b})} > 25$ GeV (ii) pseudo-rapidity smaller than $|\eta| < 2.5$. Here, the cut (ii) is required by the detector coverage for b tagging. Although we have to perform a simulation study for detailed analysis, we expect the complementary check can be available for $A_1{}^1$ with the mass up to several TeV.

Finally, we consider an alternative case that $U_u = (V_{\rm CKM})^\dagger$ and $U_d = \mathbf{1}$, and show the feasibility of discrimination of these two cases at the LHC. Fig. 4 shows the ratio of total cross sections of dielectron production via $A_1{}^1$ in each case, $\sigma_{\rm total}(U_u = (V_{\rm CKM})^\dagger)/\sigma_{\rm total}(U_d = V_{\rm CKM})$. The deviation from unity in the ratio comes from the difference of the contributions from the off-diagonal components of U_u and U_d. Fig. 2 shows that, in the case of $U_u = \mathbf{1}$ and $U_d = V_{\rm CKM}$, a subprocess with the initial state of $d + \bar{b}$ sizably contributes to the total cross section. On the other hand, in the alternative case of $U_u = (V_{\rm CKM})^\dagger$ and $U_d = \mathbf{1}$, due to the tiny distributions of t- and $\bar{t}$-quarks in a proton, the subprocesses with the initial states of $u + \bar{t}$, $\bar{u} + t$, $c + \bar{t}$, and so on give negligible contributions. Thus the ratio of total cross sections is estimated to be

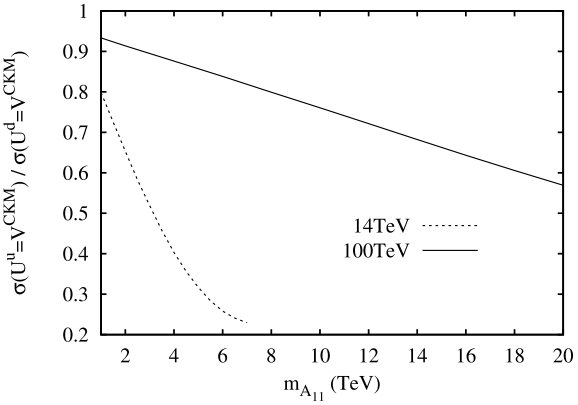

Fig. 4. The ratio of the dielectron production cross sections via $A_1{}^1$ in the two cases: (i) $U_u = (V_{\rm CKM})^\dagger$, $U_d = \mathbf{1}$ and (ii) $U_u = \mathbf{1}$, $U_d = V^{\rm CKM}$, $\sigma(U^u = V^{\rm CKM})/\sigma(U^d = V^{\rm CKM})$.

$$\frac{\sigma_{\rm total}(U_u = (V_{\rm CKM})^\dagger)}{\sigma_{\rm total}(U_d = V_{\rm CKM})} \simeq \frac{\sigma(b\bar{b} \to e^+e^-)}{\sigma(b\bar{b} \to e^+e^-) + \sigma(d\bar{b} \to e^+e^-)}, \quad (3.5)$$

which is significantly smaller than unity. Thus, the measurement of the dielectron cross section can discriminate the two cases. In addition the signals of $A_1{}^1$ flavor violating decays, e.g., $A_1{}^1 \to u\bar{t}\,(\bar{u}t)$ and $A_1{}^1 \to c\bar{t}\,(\bar{c}t)$, yield the information of U_u. The same statement is applied for the down-type quarks and U_d. To study the structure of quark mixing matrices, we need more dedicated analysis on the events with more complicated hadronic final states, which is beyond the scope of the paper.

4. Concluding remarks

In the U(3) family gauge model with twisted family number assignment (Model B) [6], the FGB $A_1{}^1$ couples to the first generation leptons, while it does to the third generation quarks. The lowest FGB $A_1{}^1$ can take a considerably smaller mass, for example, of an order of a few TeV, compared with the conventional FGB models. The direct measurement of $A_1{}^1$ at collider experiments is one of the most convincing evidences for the models with family gauge symmetry. In this paper we have argued that the most clear observable is the dielectron signal. We evaluated the production cross section and the significance of the signal for the 14 TeV and 100 TeV collision energies. At the 14 TeV and the 100 TeV collision energies with the integrated luminosity $\mathcal{L} = 3000$ fb^{-1}, the FGB with $M_{11} \lesssim 3.2$ TeV and $M_{11} \lesssim 14$ TeV is within the reach of the "evidence", respectively (see Tables 1 and 2). In order to confirm or rule out the model, a key ingredient is to check the characteristic interactions of the FGB with leptons and quarks [Eq. (2.1)]. We have evaluated the cross sections of $b\bar{b}$ ($t\bar{t}$) associated $A_1{}^1$ production, which is useful for the complementary check of the interactions with leptons and quarks. If we observe a e^+e^- peak at the LHC experiments, whether it is really a FGB or not can be checked by searching for the similar peak in $\mu^+\mu^-$ and also $\tau^+\tau^-$ modes at the same invariant mass. Measurement of the branch-

ing ratio $Br(A_1{}^1 \to b\bar{b})$ also plays an essential role in identifying whether it is really the FGB $A_1{}^1$ or not.

Finally, we would like to mention the discrimination of the family number assignment for quarks. We have two types of the assignment (see Eq. (2.4)). The different assignment gives rise to the different mass of the next lightest FGB (see Table 1 in Ref. [6]), and its decay modes are also different. However, because the next lightest FGB is predicted to be too heavy, there may be difficult to find the direct evidence at the LHC. One of the probe to the next lightest FGB is the μ–e conversion in nuclei. COMET, DeeMe and Mu2e experiments will launch soon, and search for the μ–e conversion signal [18–20]. It will be worthwhile to investigate this process to discriminate the family number assignment in the model.

In conclusion, the most clear detection of the FGB $A_1{}^1$ is to observe a e^+e^- peak at the LHC. We are looking forward to observing such a peak in the forthcoming data at $\sqrt{s} = 14$ TeV and at $\sqrt{s} = 100$ TeV.

Acknowledgements

One of the authors (YK) thanks T. Yamashita for helpful conversations and Y. Sumino for valuable comments on the U(3) family symmetry breaking scale. He (YK) also thanks H. Terazawa and I. Sogami for informing him helpful comments on works on family symmetries in earlier stage. M.Y. thanks K. Tobe for useful discussions. This work was supported in part by the Grant-in-Aid from the Ministry of Education, Culture, Sports, Science, and Technology, Government of Japan, No. 25003345 (M.Y.). The work of H.Y. was supported by JSPS KAKENHI Grant Number 15K17642.

References

[1] H. Terazawa, Y. Chikashige, K. Akama, Phys. Rev. D 15 (1977) 480;
T. Maehara, T. Yanagida, Prog. Theor. Phys. 60 (1978) 822;
P. Ramond, CALT-68-709.
[2] Y. Sumino, Phys. Lett. B 671 (2009) 477.
[3] Y. Koide, Lett. Nuovo Cimento 34 (1982) 201;
Y. Koide, Phys. Lett. B 120 (1983) 161;
Y. Koide, Phys. Rev. D 28 (1983) 252.
[4] H. Arason, et al., Phys. Rev. D 46 (1992) 3945.
[5] Y. Sumino, J. High Energy Phys. 0905 (2009) 075.
[6] Y. Koide, Phys. Lett. B 736 (2014) 499.
[7] N. Cabibbo, Phys. Rev. Lett. 10 (1963) 531;
M. Kobayashi, T. Maskawa, Prog. Theor. Phys. 49 (1973) 652.
[8] L. Randall, R. Sundrum, Phys. Rev. Lett. 83 (1999) 3370.
[9] A.L. Fitzpatrick, J. Kaplan, L. Randall, L.T. Wang, J. High Energy Phys. 0709 (2007) 013.
[10] T. Appelquist, H.C. Cheng, B.A. Dobrescu, Phys. Rev. D 64 (2001) 035002.
[11] A. Datta, K. Kong, K.T. Matchev, Phys. Rev. D 72 (2005) 096006;
A. Datta, K. Kong, K.T. Matchev, Phys. Rev. D 72 (2005) 119901.
[12] S. Matsumoto, J. Sato, M. Senami, M. Yamanaka, Phys. Rev. D 80 (2009) 056006.
[13] K.A. Olive, et al., Particle Data Group Collaboration, Chin. Phys. C 38 (2014) 090001.
[14] G. Aad, et al., ATLAS Collaboration, Phys. Rev. D 90 (5) (2014) 052005.
[15] V. Khachatryan, et al., CMS Collaboration, J. High Energy Phys. 1504 (2015) 025.
[16] A. Belyaev, N.D. Christensen, A. Pukhov, Comput. Phys. Commun. 184 (2013) 1729.
[17] H.L. Lai, et al., CTEQ Collaboration, Eur. Phys. J. C 12 (2000) 375.
[18] Y.G. Cui, et al., COMET Collaboration, KEK-2009-10.
[19] H. Natori, DeeMe Collaboration, Nucl. Phys. Proc. Suppl. 248–250 (2014) 52.
[20] L. Bartoszek, et al., Mu2e Collaboration, arXiv:1501.05241 [physics.ins-det].